Materials Horizons

Accepted Manuscript

This article can be cited before page numbers have been issued, to do this please use: K. Asselman, N. Pellens, S. Radhakrishnan, C. V. Chandran, J. Martens, F. Taulelle, T. Verestraelen, M. Hellström, E. Breynaert and C. E. A. Kirschhock, *Mater. Horiz.*, 2021, DOI: 10.1039/D1MH00733E.

ROYAL SOCIETY OF CHEMISTRY

rsc.li/materials-horizons

View Article Online
DOI: 10.1039/D1MH00733E

COMMUNICATION

Super-ions of sodium cations with hydrated hydroxide anions: inorganic structure-directing agents in zeolite synthesis

Received 00th January 20xx,
Accepted 00th January 20xx

DOI: 10.1039/x0xx00000x

Karel Asselman[†a], Nick Pellens[†a], Sambhu Radhakrishnan[a,b], C. Vinod Chandran[a,b], Johan Martens[a,b], Francis Taulelle[a,b], Toon Verstraelen[c], Matti Hellström[d], Eric Breynaert[*,a,b], Christine E.A. Kirschhock[a]

In inorganic zeolite formation, a direct correspondence between liquid state species in the synthesis and the supramolecular decoration of the pores in the as-made final zeolite has never been reported. In this paper, a direct link between the sodium speciation in the synthesis mixture and the pore structure and -content of the final zeolite is demonstrated on the example of hydroxysodalite. Super-ions with 4 sodium cations bound by mono- and bihydrated hydroxide are identified as structure-directing agents for the formation of this zeolite. This documentation of inorganic solution species acting as a templating agent in zeolite formation opens new horizons for zeolite synthesis by design.

Conceptual insights

Nature disapproves of empty spaces. So why do zeolites display cages and channels? Obviously, something occupies these voids during synthesis. In many cases, the structure-directing agents are organic cations that serve as a mould for the forming pore structure. But what takes the role of template in fully inorganic zeolite syntheses? For a long time, it has been speculated that framework charge-compensating, inorganic cations also direct the crystallisation. Nonetheless, a direct link between the speciation of inorganic cations in the synthesis mixtures and final framework remained elusive, as traditionally, zeolites are grown from chemically undefined sol and gel systems. The new concept of zeolite synthesis from hydrated silicate ionic liquids for the first time allows to clearly disclose a direct link between structure in synthesis solution and formed zeolite crystals. In this case study, sodium super-ions have been identified as most probable suspects to template the hydroxysodalite structure.

Organic molecules and cations are well-known for their templating role in the synthesis and transformation of zeolites[1-7]. Stable organic molecules, exhibiting known and predictable conformations during zeolite synthesis, have been used as pore-filling structure-directing agents, representing a leap towards zeolite synthesis by design[8,9]. Yet, in inorganic zeolite syntheses, a dynamic and complex interplay between metal cations, anions, water, and sources of zeolite framework atoms (T-atoms) defines the outcome. Breck suggested a structure-directing role of inorganic species such as metal cations as early as 1964[10]. But except for zeolite transformations[1], a structure-directing function of inorganic cations has not yet been proven. Demonstrating such mechanisms in inorganic synthesis would represent a major milestone towards the rational design of zeolites, exploiting cheap inorganic ions instead of costly and sacrificial structure-directing organics. It is accepted that zeolite formation is solution-mediated[11]. If inorganic species fulfil a pore-filling and templating role, it should be possible to observe links between dissolved species and supramolecular assemblies decorating the pores of the as-made final zeolites, similarly to what has been observed for organic templates[12].

Unfortunately, inorganic zeolite syntheses usually occur in complex systems containing colloids or gels. This impairs detailed elucidation of the local speciation in the synthesis medium, obscuring the connections between species in the synthesis and the final zeolite. The present work exploits hydrated silicate ionic liquids (HSILs)[13,14] - true homogeneous fluids containing hypohydrated, cation-stabilized (alumino)-silicate oligomers – as the source of T-atoms for zeolite synthesis. The low water content, in combination with the excess of alkali metal hydroxide, prevents the formation of gels, sols, or colloids. HSILs allow detailed exploration of their chemistry and speciation, offering opportunities to link the inorganic speciation in the zeolite precursor liquid with the pore content of the final zeolite. Comparing the prevailing speciation in solution with the cage decorations in the final zeolite should allow conclusions on structure-directing effects of specific

[a] COK-Kat, KU Leuven, Celestijnenlaan 200F, 3001 Heverlee, Belgium
[b] NMRCoRe, KU Leuven, Celestijnenlaan 200F, 3001 Heverlee, Belgium
[c] Center for Molecular Modelling (CMM), Ghent University, Technologiepark 903, B-9052 Ghent, Belgium
[d] Software for Chemistry and Materials B.V., 1081HV Amsterdam, The Netherlands
† Shared first authors with equal contributions to this work
* Corresponding author
Electronic Supplementary Information (ESI) available: [details of any supplementary information available should be included here]. See DOI: 10.1039/x0xx00000x

inorganic species. This manuscript highlights experimental and computational evidence, revealing a clear link between the ionic structures present in the zeolite synthesis liquid and the extraframework species in hydroxysodalite crystallising from it. Similar connections might be found in many inorganic zeolite syntheses, provided sufficient knowledge on the complex solution chemistry in these systems becomes available. Hydroxy- or basic sodalite is a well-known zeolite shown to be the primary product in all common sodalite syntheses[15]. Hydroxysodalite is reported to form in a wide range of SiO_2/Al_2O_3 synthesis ratios in the Si-Al-Na phase diagram, with molar NaOH concentrations up to 22M[16]. In absence of other anions than hydroxide, sodalite frameworks always form as hydroxysodalite. From those, non-basic sodalites can only be obtained from post-synthetic extraction of NaOH[15,17-19]. As the name suggests, hydroxysodalite contains hydrated hydroxide anions that compensate for the charge of excess sodium cations in the zeolite cages, leading to the ideal chemical unit cell composition $Na_8Si_6Al_6O_{24}(OH^-)_2.2H_2O$. In the hydroxysodalite structure described in literature, the hydroxide anions occur in geometries reminiscent of Zundel anions, monohydrated hydroxide anions. This anion has been suggested to be a transient species in aqueous hydroxide solutions and even in pure water[20,21]. Its presence in the pores of hydroxysodalite suggests a strong correlation between this zeolite framework and its pore content during synthesis. Hydroxysodalite synthesis relies on hyper-alkaline conditions and on the exclusive presence of NaOH next to water and (alumino)silicate oligomers[22]. Such conditions are accessible using true liquid HSIL zeolite synthesisfluids[13], prompting to explore the compositional range and corresponding ionic structures in those HSILs, forming hydroxysodalite.

In zeolite syntheses, the hydroxide content usually is expressed as the ratio of SiO_2/NaOH, which is inversely proportional to the alkalinity. Another important, but less explored, variable in inorganic zeolite synthesis is the water content, here represented by the relative cation hydration H_2O/NaOH. Both ratios refer to the nominal amounts of silicate, water, and hydroxide added to the synthesis mixture, and hence do not represent the *ad hoc* ratio occurring during synthesis. The latter is a function of the oligomeric speciation of T-atoms in the synthesis mixture. At room temperature, HSILs based precursor liquids are in chemical equilibrium, allowing usage of their nominal composition for parametrization of a given system. In this work, the sample SiO_2/NaOH ratio and relative cation hydration H_2O/NaOH were varied between 0.1 – 0.5 and 3 – 10, respectively. Using fixed molar amounts of silicon and aluminium, the water and sodium hydroxide content in the synthesis liquids was varied, generating a series with composition of 0.5 SiO_2 : 0.013 Al_2O_3 : x NaOH : y H_2O, x and y ranging between 1 - 5, and 3.75 – 15, respectively. Full details on the syntheses can be found in the ESI. As shown in Fig. 1 and in Table S1 and Fig. S1, phase pure sodalite exclusively forms in

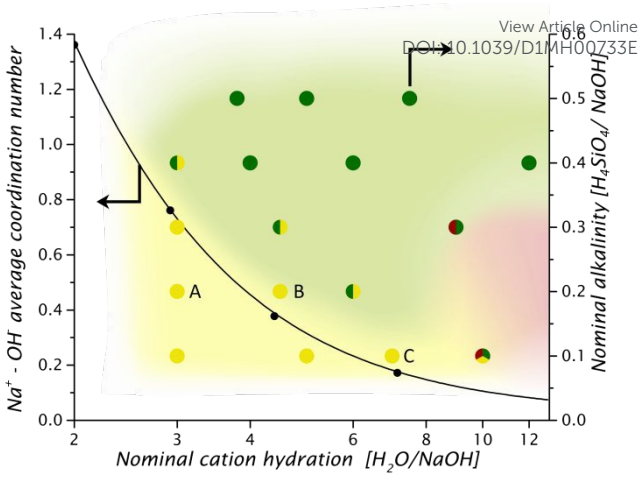

Fig. 1: Synthesized frameworks in the 0.5 SiO_2 : 0.013 Al_2O_3 : x NaOH : y H_2O system at 60°C (circles) compared to speciation in solution (black dots and line). Right y-axis: Phase pure hydroxysodalite (yellow) is only produced at low cation hydration and low Si/OH^-. Other conditions form GIS-type zeolite (green) and traces of FAU (red). Left y-axis: Sodium hydroxide solution chemistry according to Hellström et al[27]. Direct Na^+ - OH^- coordination becomes relevant below the transition region between SOD and GIS zeolite formation. Samples A,B, and C with nominal hydration numbers of 3, 4.5, and 7 are discussed in detail in the text.

mixtures combining high alkalinity (SiO_2/NaOH < 0.4) with low cation hydration numbers (H_2O/NaOH < 7). In line with observations reported by Maldonado *et al.,* crystallizing phase pure hydroxysodalite in systems with increased cation hydration also requires increased alkalinity.[22] With increasing dilution, literature reports the formation of faujasite (FAU)-type zeolite at 60°C. But in the present study, using HSILs, gismondine (GIS)-type zeolite formed at higher water content and/or lowered alkalinity. Only in samples with high hydration ratios (H_2O/NaOH>9), FAU was observed as a minority phase in the powder X-ray diffraction patterns. GIS is usually obtained at synthesis temperatures above 100°C and known as a typical transformation product of FAU[22]. The rather unexpected observation of GIS at 60°C most probably results from the use of hydrated silicate ionic liquids, where high alkalinity leads to a high solubility of FAU-type zeolite[1].

ICP analysis of all sodalites showed a 1:1 [Si/Al] ratio. Intriguingly, this high-aluminium framework is obtained from precursor liquids with $[Si/Al]_{liquid}$ of 20, highlighting the important role of Al-containing species for zeolite formation in HSILs, and in traditional aluminosilicate zeolite synthesis in general[13,23]. ICP analysis further demonstrated all sodalite samples exhibited a Na/Al ratio exceeding 1, thereby indicating them as hydroxysodalites ($Na_{6+x}[Al_6Si_6O_{24}](OH^-)_x.yH_2O$). Three samples crystallised in conditions with varying nominal cation hydration, indicated as A, B and C in Fig. 1, were selected for further detailed structural analysis by NMR crystallography, combining advanced NMR methods with diffraction and modelling[24-26].

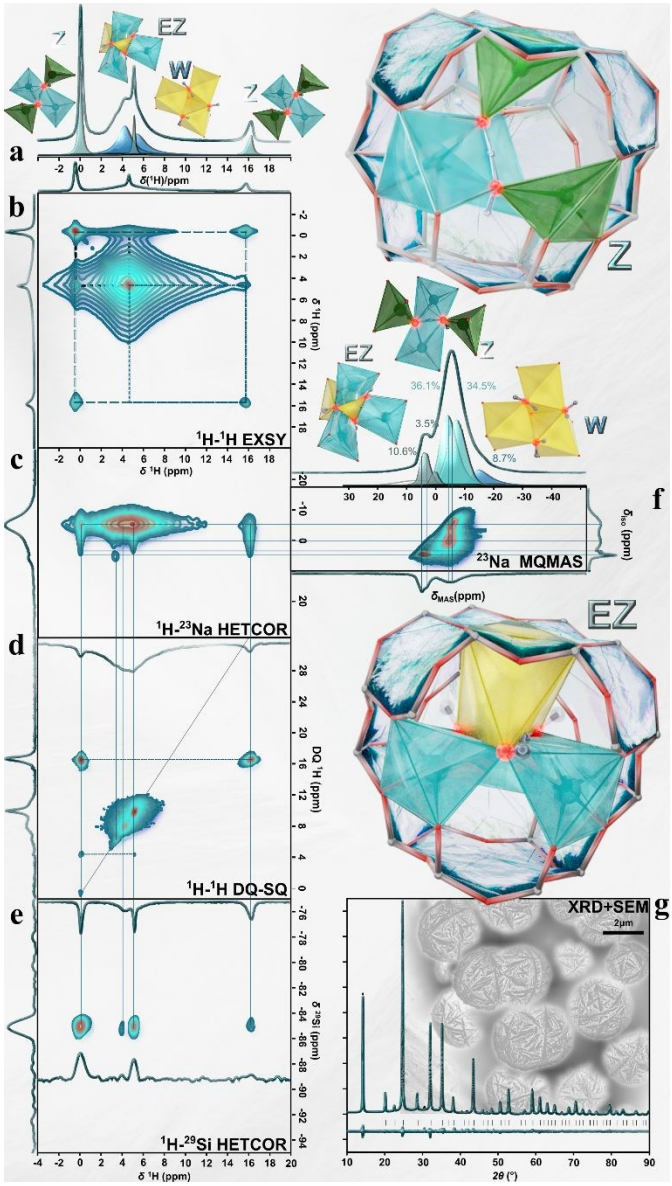

Fig. 2: (a) ^{1}H NMR and its spectral decomposition revealing the Zundel, extended Zundel and water cage protons in hydroxysodalite (sample B); (b) ^{1}H EXSY showing proton chemical exchange; (c) ^{1}H-^{23}Na HETCOR (d) ^{1}H-1H DQ-SQ correlation; (e) ^{1}H-^{29}Si HETCOR; (f) ^{23}Na 3QMAS and (g) X-ray diffractogram and SEM; All NMR spectra were acquired at 253K. The structures of hydroxysodalite cages with Zundel (Z), Extended Zundel (EZ) anions, i.e. two water molecules next to one hydroxide and 4 Na^+ ions and sodium – water cages (W). Polyhedra in green indicate 4-fold, in cyan 5-fold, and in yellow 6-fold sodium coordination.

The sodalite topology entirely consists of face-sharing sodalite cages. In stoichiometric hydroxysodalite with formula $Na_8[Al_6Si_6O_{24}](OH^-)_2.2H_2O$, each of those β-cages contains a tetrahedron of four Na^+ cations, located on the three-fold axes of the cubic unit cell, forming a $[Na_4(H_3O_2)]^{3+}$ super-ion with a central Zundel type $H_3O_2^-$ anion, as a shared edge between 2 of the 4 cations (Fig. 3 Z cage). Each of the Na cations in this super-ion further coordinates to three framework oxygen atoms of a six-ring window of the cages at an approximate distance of 2.4 Å (Fig. 3 Z). Detailed structure analysis of sample B revealed the presence of the Zundel type anion by the combination of ^{1}H, ^{1}H EXSY and ^{1}H DQ-SQ MAS NMR (Fig. 2, a,b,d). The two ^{1}H resonances at 16.3 and 0.1 ppm, respectively, represent two types of inequivalent protons in close proximity, evident from the double quantum correlations (Fig. 2d) and in chemical exchange (Fig. 2b). They can be assigned as the central and exterior protons of the Zundel anion, respectively. Whether or not the proton in the Zundel-like $[H_3O_2]^-$ is located exactly in the centre between the shared edge between polyhedra is in the context of this work not relevant, as ^{1}H-NMR shows strong chemical exchange, which implies the super-ion is dynamic in terms of its central and external protons. Samples A and C exhibited similar 1D ^{1}H NMR spectra as sample B, but with the different spectral components present in different ratios. Sample A was further characterized by FT-IR and TGA (Fig. S18-20), confirming the vibration signature of a Zundel like species and revealing a weight loss upon calcination in agreement with the corresponding chemical composition. The structure of the $[Na_4(H_3O_2)]^{3+}$ super-ion was also confirmed by X-ray diffraction with Rietveld refinement in all three samples. The coordination polyhedra of the sodium cations and Zundel anion (Z) are visualized in Fig. 3, an animation for clearer view is provided as supplement (movie S1). The sodium cations in the super-ion have coordination numbers of 4 or 5, shown in green and cyan, respectively. Their geometries resemble distorted corner-sharing seesaw (CN = 4) and edge-sharing square pyramid (CN = 5) polyhedra[27]. The structure of the $[Na_4(H_3O_2)]^{3+}$ super-ion shows the solvation shell of sodium in these cages to be completely substituted by non-water ligands. All four sodium cations, two by two inequivalent (Fig. 3, Z-cage), interact with the Zundel anion as indicated both by the ^{1}H-^{23}Na HETCOR and ^{1}H{^{23}Na} TRAPDOR spectra (Fig. 2c, pane ^{1}H-^{23}Na HETCOR and Fig. S8). X-Ray diffraction with Rietveld refinement localizes these Na^+ ions within bonding distance of the Zundel anion oxygen atoms, with 2 Na^+ ions coordinating both oxygen atoms while the other two coordinate to only one of them (Fig. 2g). The two oxygen atoms of the Zundel anion are at a close distance of 2.3 Å, in full agreement with a previous neutron diffraction study of hydroxysodalite, identifying the average position of the H-bonding deuterium atom almost centred between these oxygen atoms, implying strong hydrogen bonding[17,28,29]. This leads to unusually small angles ∠O–Na–O of 50.2° and remarkably short bond lengths between Na^+ and oxygen, ranging between 2.33 and 2.98 Å. The observed crystallographic symmetry implies the Zundel anion shows orientation disorder across the 12 possible equivalent sites around the centre of the β-cage[17]. This is in agreement with our NMR results, and the very small rotation barrier of 7.6 kcal/mol determined by molecular simulation (ESI section 1.5), both implying dynamic disorder. A visualisation of the interchange of polyhedral is provided as supplement (movie S2) At first sight, the Rietveld refinement of the powder diffractograms of samples A, B and C did not immediately reveal any presence of cage decorations differing from the above described Zundel-sodium super-ion. The 1D direct excitation ^{23}Na MAS NMR spectra of the samples, however, show distinct extra Na

View Article Online
DOI: 10.1039/D1MH00773G

resonances which cannot be assigned to Z-cages, which indicates occurrence of other cation-ligand configurations (Fig. 3 EZ, W).

Inspecting the ^{1}H-^{23}Na HETCOR spectrum (Fig. 2c, sample B), and correlating it with the ^{23}Na 3QMAS (Fig. 2f) and the ^{1}H DQ-SQ (Fig. 2d) spectra, instantly reveals correlations between the various Na and H species. The two dominant Na resonances assigned to the Z-configuration, with peak maxima at -7 ppm (isotropic chemical shift, δ_{iso}= -6 ppm; quadrupole coupling constant, C_Q = 0.9 MHz) and -4 ppm (δ_{iso}= -2 ppm; C_Q = 1.3 MHz), each correlate with the external and central Zundel protons exhibiting ^{1}H signals at 0.1 and 16.3 ppm, respectively. The Na species with δ_{iso}= -6 ppm also correlates to two additional ^{1}H resonances at 5.1 (sharp) and 4 (broad) ppm, respectively. Both ^{1}H resonances exhibit a self-correlation in the ^{1}H DQ-SQ spectrum and consequently can be assigned to water molecules, present in the neighbourhood. Sodium, represented by the broad signal with a peak maximum at -15 ppm (δ_{iso}= -12.3 ppm; C_Q = 1.7 MHz), is attributed to W-cages containing 3 sodium ions and 4 water molecules, in agreement with the assignment of Engelhard[15]. The decomposed ^{23}Na spectrum further shows two ^{23}Na resonances in a 3:1 ratio, both exhibiting a second order quadrupolar pattern that can be described with the following parameters: (i). (δ_{iso}) = +6.2 ppm, (C_Q)= 1.3 MHz, asymmetry parameter (η_Q = 0.49), and (ii). δ_{iso} = +2.4 ppm, C_Q= 1.2 MHz, η_Q = 0.53, respectively. Both signals correlate to ^{1}H resonances with chemical shifts at 3 ppm and 5.1 ppm, which, according to their self-correlation in the ^{1}H DQ-SQ spectrum, also are assigned as water molecules. The water molecules showing ^{1}H resonance with a chemical shift at 5.1 ppm also demonstrate double quantum correlations with the external ^{1}H of the Zundel ion (0.1 ppm). This indicates the existence of an assembly similar to Z-cages but extended by an extra water molecule, i.e. a super-ion consisting of a bihydrated hydroxide ion and 4 sodium ions (EZ). In summary, the NMR reveals multiple types of possible cage decorations, clearly identifying the presence of EZ and W cages next to the dominant Z-configuration. ^{1}H-^{29}Si HETCOR spectrum (Fig. 2e) further confirms that the different ^{1}H populations corresponding to different Na^+ ion organizations, i.e. Z (δ(^{1}H) 0.1 and 16.3 ppm), EZ (δ(^{1}H) 3 & 5.1 ppm) correlate to the same Si distribution so that it is clear the three different arrangements are present within the same crystal. This observation is in agreement with Engelhardt et al. who also described different cage decorations in the same sample, i.e. the Zundel-sodium super-ion (Z cage) next to cages with sodium ions and water (W cage) in varying degrees[15]. While it was then assumed the W cages arise from post-synthetic washing, in our case we observe W cages directly after synthesis. This is not very surprising, as even in our concentrated sodium hydroxide solutions, a limited fraction of free water molecules is present[27], allowing occasional expression of W cages (vide infra). In the current study, yet a third type of cage decoration has been identified, earlier proposed by Felsche et.al.[30], where two water molecules are present next to one hydroxide and 4 sodium ions (EZ). NMR analysis of all three samples A, B, C (Fig. S6-15, Table S5-8), allowed quantification of the fractions of Water cages, Extended Zundel cages and Zundel cages, which in our case occur as solid solutions within the crystals. The sample with the lowest cation hydration (sample A) contained 74% and 22% of Z and EZ cages, respectively, but negligible numbers of water cages. Increasing nominal hydration numbers to 4.5 and 7 in samples B and C led to increasing numbers of EZ and W cages (Table 1), correlating the increased water content of the synthesis mixture to the cage decoration. Based on the identification of the 3 different cage contents by NMR, theoretic modelling and analysis of the electron density maps derived from Rietveld analysis of the samples, the spatial arrangements of water and hydroxide ions in EZ and W cages could be deduced and refined (ESI section 1.3, Fig. S2-4, Table S2-4). Sample A, containing almost no W-cages served to determine the position of the extra water molecule, which also was confirmed by molecular modelling (Fig. S16). The resulting super-ion $(Na_4(H_5O_3))^{3+}$ is quite similar to the structure found in Z-cages, but here all sodium ions participate in edge-sharing, where each edge is formed by a Zundel-anion like configuration. This results in one sodium in distorted octahedral coordination, sharing each of the three edges of one face with one sodium in square bi-pyramidal coordination. With this information on the

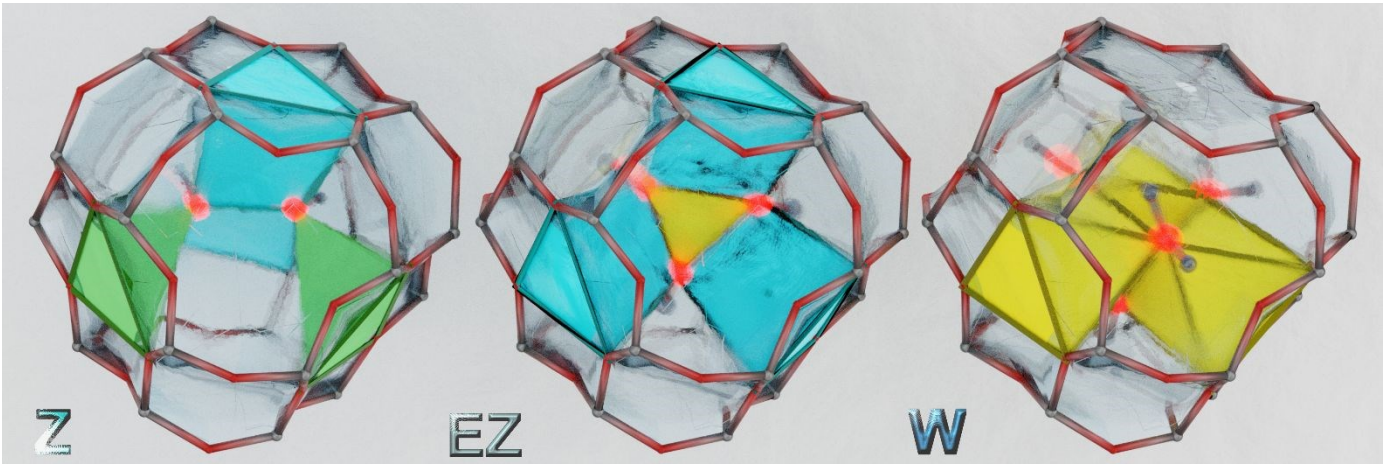

Fig. 3: Visualization of Z (left), EZ (middle) and W (right) configurations in the sodalite cage.

Table 1: Comparison of cage decoration derived by ^{23}Na NMR and XRD.

Sample	*A*		*B*		*C*	
[H_2O]/[NaOH]	3		4.5		7	
[Si]/[NaOH]	0.2		0.2		0.1	
	NMR	*XRD*	*NMR*	*XRD*	*NMR*	*XRD*
%Z cages	73.8	77.2	73.3	74.1	55.6	56.1
%EZ cages	22.4	21.7	14.6	13.8	23.6	22.7
%W cages	3.8	1.1	12	12.1	20.8	21.2
Avg. Na^+ CN	4.7		4.8		5.0	

exact structure of Z and EZ cages, from samples B and C the configuration of cations and water in the W-cages then was determined. Here, the three sodium ions are all found in identical edge-sharing octahedral coordination. Finally, the obtained structures of all three cage types served for Rietveld refinement of the powder X-ray data (ESI section 1.3). The obtained occupation numbers were used to derive the percentage of cages of each type, which resulted in excellent agreement with the quantitative observation by NMR (Table 1). This correspondence between XRD and NMR served as final confirmation of the accuracy of the used structure models. The present study reveals the relative amounts of the three cages present in hydroxysodalite from different HSIL compositions depend on nominal water content during synthesis, confirming that in all cases the fraction of cages with Zundel anions is the highest.

Next, we demonstrate, that hydroxysodalite only forms from those liquids, where sodium super-ions with shared edges, made up of hydrogen-bonded, hydrated hydroxide ions, exist in significant concentration. As shown earlier, the precursor liquids of hydroxysodalite are all characterised by high alkalinity (SiO_2/NaOH < 0.3) and strictly limited water content (H_2O/NaOH < 7). Naturally, zeolites do not form in pure NaOH solutions, as the presence of T-atoms is necessary. However, in the present study, the T-atom molar fraction is as low as 0.0127 and still result in the synthesis of high-quality hydroxysodalite. McCormick et. al. show that at such low silicate concentrations ([SiO_2]/[NaOH] < 0.5), silicate does not affect the sodium speciation compared to pure NaOH solutions[31]. This implies that the states of Na^+ in the studied hydroxysodalite-producing mixtures are equivalent to concentrated aqueous NaOH solutions. Therefore, it is valid to derive the formation and stability of edge-sharing super-ions in hydroxysodalite precursor liquids from the sodium coordination chemistry in concentrated aqueous NaOH. Based on molecular dynamics simulations, Hellström et al. and Megyes et al. confirmed that at diluted NaOH concentrations, sodium preferably coordinates 5-6 water molecules[27,32]. However, when water is severely limited, sodium turns to non-water ligands, in absence of other options. Specifically, it turns to hydrogen-bonded hydroxide, i.e. Zundel type anions[20,21,27] to complete its coordination shell. This gives rise to a wide variety of distorted coordination structures with much shorter Na-O distances[32]. With decreasing water content, the number of water ligands decreases from 6 down to 5 and eventually to 4. This lack of coordination water forces Na cations also to share ligands, by forming corner- and edge-sharing configurations. In parallel, the number of coordinated hydrated hydroxide ions increases[27] (Fig. 1). Theoretical modelling of highly concentrated NaOH solutions has shown the occurrence of species in solution, which are typically observed only in crystalline sodium hydroxide-hydrates[27,33]. Among those are the distorted seesaw and the square pyramid polyhedra, being the most stable species for coordination numbers 4 and 5, respectively. In these species, experimentally observed in solid-state and in silico models of highly concentrated NaOH solutions, bond lengths can be significantly reduced to 2.4-2.5 Å[27,32]. This is in line with the work of Merchant et al. who demonstrated that lower coordination numbers go along with decreasing Na-O bonding distances[34]. As mentioned before, and shown in Fig. 1, direct Na-OH interactions gain significance when the presence of water is severely limited[27], i.e. exactly the region where hydroxysodalite is synthesized. Another feature of limited water is the increasing occurrence of H-bonding between ligands of the same central cation (Fig. S17), leading to small ∠O-Na-O (50°-60°) angles, not observed in dilute systems but inevitably found in the cages of hydroxysodalite. Noteworthy for highly concentrated NaOH solution also is the higher preference for edge-sharing of square pyramidal polyhedra in comparison to the seesaw configuration. Simulations at the solubility limit of NaOH indicate that at any given moment, as much as 80% of all ligands in Na^+ coordination complexes are shared at least between two polyhedra and, on average, coordinate 1 Zundel-like anion[27,29]. Therefore, only when dehydration effects stabilize corner- and edge-sharing configurations, resulting in shorter Na-O distances and reduced ∠O-Na-O bond angles, Zundel anions and water can form an edge between two neighbouring sodium polyhedra, e.g. in square pyramidal or higher coordination, and only from those liquids hydroxysodalite forms.

Combined, these results directly imply that the observed super-ions found in Z and EZ cages of hydroxysodalite (Fig. 1 and 3) on average exist at any time in their room temperature precursor liquids. As mentioned before, in hydroxysodalite, the Na^+ coordination polyhedra are short-lived and dynamically interchange between the twelve crystallographic equivalent positions[17] (Fig. 3, movie S2), similar to the highly dynamic interchange of polyhedral units observed in concentrated NaOH[27]. Nonetheless, with the increasing density of the polyhedral network in NaOH solutions, the probability of a configuration of four sodium ions in edge- and corner-sharing arrangement is high and consistent with the presence of the super-ions observed in the Z and EZ sodalite cages. It is pointed out, however, that the exact configurations of the polyhedral enclosed in hydroxysodalite (Z, EZ cages), in solution are in constant dynamic exchange [27,35].

View Article Online
DOI: 10.1039/D1MH00733E

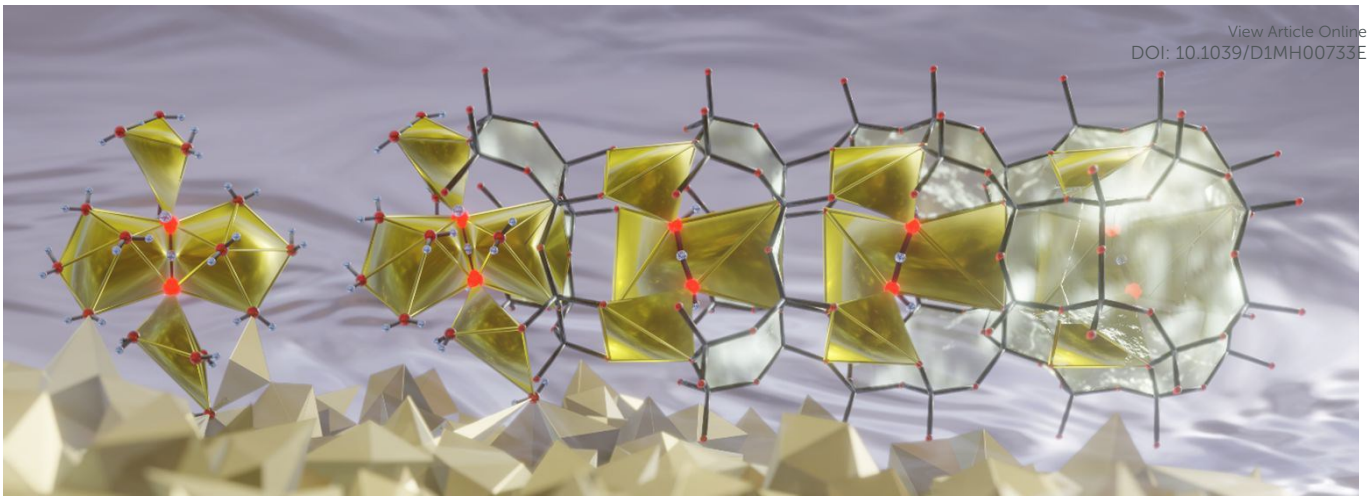

Fig. 4: Illustration of the sodalite framework emerging in concentrated NaOH solution by dynamic substitution of water -and/or hydroxide ligands with aluminosilicate species. Coordination polyhedra all shown in yellow as dynamic exchange between geometries occurs in liquid state, as well as within the product.

Based on the above reflections on the structures of the hydroxysodalites and their synthesis mixtures, it is proposed that a substitution of aquo- and hydroxo-ligands of edge and corner-sharing sodium complexes by aluminosilicate successively results in the prevalent order, visualized in Fig. 4. For the expression of a sodalite cage by subsequent ligand exchange for framework atoms, a local assembly of four sodium ions dynamically interchanging edge- and corner-sharing is necessary, a situation only encountered at high NaOH concentrations. The oxygen atoms, provided by aluminosilicate oligomers, then can seamlessly participate in the polyhedral network, resulting in the occlusion of the described super-ions in the cages of the forming zeolite. Consequently, the finally achieved cage decorations mirror the local coordination environment during the formation of the respective sodalite cage. In the case of the Z-cage, the corresponding super-ion $[Na_4(H_3O_2)]^{3+}$, displays an average coordination number of 4.5, which for the EZ cage increases to 5.25 and finally to 6 for the W-cage. The coordination number averaged over the fractions of the various cages in the three samples is in perfect agreement with the trend of the global coordination number of sodium in the respective synthesis fluid with increasing hydration (Table 1). This readily explains the increasing fractions of EZ and W cages with increasing hydration of the synthesis HSIL. Furthermore, the employed synthesis temperature does not seem to play a significant role in the cage type population distributions and is expected to mainly influence dynamics. With increasing water content, simulations show that the probability of direct Na-OH coordination leading to edge-sharing polyhedra strongly diminishes, eventually becoming close to negligible for $H_2O/NaOH > 8$.[27] This corresponds to synthesis conditions where hydroxysodalite does not form, but GIS or FAU-GIS mixtures crystallize instead. The transition from SOD to these other frameworks shifts to lower $H_2O/NaOH$ ratios as the Si/NaOH ratio increases (Fig. 1). This makes sense, as a larger portion of hydroxide is involved in aluminosilicate deprotonation and oligomerisation. This leads to increased cation hydration levels, which in turn decreases the concentration of OH^--ligands, involved in edge-sharing. This further strengthens the notion that active participation of Zundel-like anions in Na^+ coordination is a prerequisite for hydroxysodalite crystallization. The structural resemblance between a combination of polyhedra commonly occurring in NaOH solutions and the configuration of the Z and EZ super-ion complexes in hydroxysodalite is striking and represents a direct link between the solution-state chemistry of zeolite synthesis liquids and the charge-balancing species contained in the pores of a crystallizing zeolite. The coincidence of the region of formation of hydroxysodalite with the region of existence of Zundel anion - sodium cation complexes suggests these super-ions as true structure-directing agents in zeolite formation. Note that the proposed template function of the Zundel-anion-sodium assemblies also explains why post-synthesis exposure to water converts hydroxysodalite (Z, EZ cages) to hydrated sodalite (W cages)[15]. Intimate Na^+-OH^- ionic interactions are not stable in dilute, aqueous solutions and as a result, prolonged exposure to water leads to NaOH leaching from the cages. This observation was tested in a final experiment to prove the structure-directing role of the edge-sharing super-ion complexes (ESI section 2.8, Fig. S21-22): Exposure of sample A to pure water for 1 week at room temperature revealed the formation of small amounts of hydrosodalite next to remaining hydroxysodalite, as evidenced by XRD. Only after further 3 weeks at 60°C most excess Na-, and OH- ions could be leached from the structure, resulting in almost pure hydrosodalite. This proves that sodium cations and hydroxide ions are mobile in the zeolite framework. In theory, this mobility also enables the option that hydroxysodalite could be formed by diffusion of excess sodium hydroxide into the cages of hydrosodalite, driven by the high concentration of the synthesis fluid. Interestingly, literature describes the removal of NaOH from hydroxysodalite as an irreversible process, where any reconversion of hydrosodalite into hydroxysodalite in concentrated NaOH solutions proceeds through a dissolution precipitation

reaction[18-19]. We confirmed the formation of hydroxysodalite by templation rather than by diffusion of NaOH into a hydrosodalite structure by immersing the hydrosodalite sample, obtained by leaching the excess ions, in sodium hydroxide solutions with the same concentrations as those used in the HSIL from which it was crystallised. Even after more than two weeks at room temperature, there is no sign of any reconversion to hydroxysodalite, proving that super-ions consisting of 4 sodium ions and hydrated hydroxide anions must have been included in the cages during cage formation, implicating templation by the $[Na_4(H_3O_2)]^{3+}$ and $[Na_4(H_5O_3)]^{3+}$ super-ions as the mechanism for hydroxysodalite formation. Only in fluids where those super-ions dynamically exist, the sodalite framework can be formed.

The dynamic and short-lived nature of superionic structures such as $[Na_4(H_3O_2)]^{3+}$ does not impede their structure-directing function. Crystallisation processes always involve transient density fluctuations resulting in the temporary local occurrence of ordered organisations exceeding the solubility of the crystals being formed. This directly implies also dynamic and short-lived species can serve as templates and become part of the final crystals. Since hydroxysodalite formation is a crystallisation process, any transient species can be templating as long as its lifetime is of the same order of magnitude than that of the density fluctuation enabling the crystallisation. The here identified sodium-super-ions consequently satisfy all requirements to be identified as true templates in zeolite formation: Hydroxysodalite only forms in their presence, their increased concentration leads to fast nucleation, and they are found in the zeolite after crystallisation.

Such close correspondence between solution species and pore-filling in zeolites provides a direct connection between solvated species in zeolite synthesis liquids and the final zeolite structure. Up to now, such correlations were reserved for the description of organic structure-directing agents. This work implies that knowledge of the inorganic speciation in zeolite synthesis could lead to the 'rational' use of cation coordination chemistry to exploit inorganic structure-directing species for zeolite frameworks. Hydrated Silicate Ionic Liquids (HSILs) make future research to further explore this concept in more detail highly feasible. Asides from offering the option to stepwise study zeolite formation in inorganic systems, the HSIL methodology also offers a new horizon for sustainable SDA-assisted zeolite synthesis. Given the specific stability regions of these coordination complexes, change, removal, and recycling of the inorganic structure-directing agents can be achieved by chemistry induced stability changes, instead of sacrificial removal of the template via calcination as is the case for most organic structure-directing agents.

Conflicts of interest

There are no conflicts to declare.

Acknowledgements

View Article Online
DOI: 10.1039/D1MH00733E

This work was supported by the Hercules Foundation (AKUL/13/21), by the Flemish Government, department EWI via the Hermes Fund (AH.2016.134). J. A. M. and C.E.A.K. acknowledge the Flemish Government for long-term Methusalem structural funding. K.A., N.P., T.V, E.B. and C.E.A.K. acknowledge joined funding by the Flemish Science Foundation (FWO) (1.5.061.18N and G083318N). This work has received funding from the European Union's Horizon 2020 research and innovation programme under grant agreement no. 798129 and from the European Research Council (ERC) under grant agreements no. 834134 (WATUSO).

Notes and references

1 L. Van Tendeloo, E. Gobechiya, E. Breynaert, J. A. Martens and C. E. A. Kirschhock, *Chem. Commun.*, 2013, **49**, 11737–11739.
2 K. Iyoki, Y. Kamimura, K. Itabashi, A. Shimojima and T. Okubo, *Chem. Lett.*, 2010, **39**, 730–731.
3 C. E. A. Kirschhock, E. J. P. Feijen, P. A. Jacobs and J. A. Martens, in *Handbook of Heterogeneous Catalysis*, Wiley-VCH Verlag GmbH & Co. KGaA, Weinheim, Germany, 2008, pp. 160–178.
4 A. Nearchou and A. Sartbaeva, *CrystEngComm*, 2015, **17**, 2496–2503.
5 D. Jo and S. B. Hong, *Angew. Chemie*, 2019, **131**, 13983–13986.
6 A. Corma, F. Rey, J. Rius, M. J. Sabater and S. Valencia, *Nature*, 2004, **431**, 287–290.
7 G. Wang, B. Marler, H. Gies, C. A. Fyfe, P. Sidhu, B. Yilmaz and U. Müller, *Microporous Mesoporous Mater.*, 2010, **132**, 43–53.
8 Z. Wang, J. Yu and R. Xu, *Chem. Soc. Rev*, 2012, 41, 1729-1741.
9 S. Li, J. Li, M. Dong, S. Fan, T. Zhao, J. Wang and W. Fan, *Chem. Soc. Rev*, 2019, 48, 885-907.
10 D.W. Breck, *J. Chem. Educ.*, 1964, 41(12), 678-689.
11 C.S. Cundy and P.A. Cox, *Microporous Mesoporous Mater.*, 2005, 82(1-2), 1-78.
12 M. Moliner, F. Rey, A. Corma, *Angew. Chem.*, 2013, 52, 13880-13889.
13 L. Van Tendeloo, M. Haouas, J.A. Martens, C.E.A. Kirschhock, E. Breynaert, F. Taulelle, *Faraday Discuss.*, 2015, 179, 437-449.
14 M. Houlleberghs, E. Breynaert, K. Asselman, E. Vaneeckhaute, S. Radhakrishnan, M. W. Anderson, F. Taulelle, M. Haouas, J. A. Martens and C. E. A. Kirschhock, *Microporous Mesoporous Mater.*, 2019, **274**, 379–384.
15 G. Engelhardt, J. Felsche, P.B. Kempa, P. Sieger and P. Fischer, *J. Am. Chem. Soc*, 1992, 114 (4), 1173–1182.
16 W. Fan, K. Morozumi, R. Kimura, T. Yokoi and T. Okubo, *Langmuir*, 2008, 24(13), 6952–6958.
17 M. Wiebcke, G. Engelhardt, J. Felsche, P.B. Kempa, P. Sieger, P. Fischer, *J. Phys. Chem.*, 1992, 96, 392-397.
18 B. Subotić and L. Sekovanić, *J. Cryst. Growth*, 1986, **75**, 561–572.

View Article Online
DOI: 10.1039/D1MH00733E

19 B. Subotić, D. Škrtić, I. Šmit and L. Sekovanić, *J. Cryst. Growth*, 1980, **50**, 498–508.
20 M.E. Tuckerman, D. Marx and M. Parrinello, *Nature*, 2002, 417, 925-929.
21 R. Pang, D.Y. Wu and Z.Q. Tian, *AIP Conference Proceedings*, 2010, 1267, 746-747.
22 M. Maldonado, M.D. Oleksiak , S. Chinta, J.D. Rimer, *J. Am. Chem. Soc*., 2013, 135, 2641–2652.
23 T.W. Swaddle, *Coord. Chem. Rev.*, 2001, 219-221, 665-686.
24 M. Houlleberghs, A. Hoffmann, D. Dom, C. E. A. Kirschhock, F. Taulelle, J. A. Martens, E. Breynaert, *Anal. Chem.*, 2017, 89, 13, 6940-6943
25 S. Radhakrishnan, H. Colaux, C. V. Chandran, D. Dom, L. Verheyden, F. Taulelle, J. Martens, E. Breynaert, *Anal. Chem.*, 2020, 92, 19, 13004 – 13009
26 D. L. Bryce, F. Taulelle, *Acta. Cryst*., 2017, C73, 126-127
27 M. Hellström, J. Behler, *Phys. Chem. Chem. Phys*, 2017, 19(1), 82-96.
28 A. Koizumi, K. Suzuki, M. Shiga and M. Tachikawa*, J. Chem. Phys*., 2011, 134, 031101.
29 K. Abu-Dari, K.N. Raymond, D.P. Freyberg, *J. Am. Chem. Soc*., 1979, 101(13), 3688–3689.
30 J. Felsche and S. Luger, *Thermochimica Acta*, 1987, 118, 35-55
31 A. V. McCormick, A. T. Bell, and C. J. Radke, *J. Phys. Chem*., 1989, 93(5), 1733–1737.
32 T. Megyes, S. Bálint, T. Grósz, T. ´Radnai and I. Bakó, *J. Chem. Phys.,* 2008, 128(4), 044501
33 J.R. Rustad, A.R. Felmy, K.M. Rosso, E.J. Bylaska, *American Mineralogist*, 2003, 88(2-3), 436-449.
34 S. Merchant and D. Asthagiri, *J. Chem. Phys*., 2009, 130, 195102.
35 M. Hellström, M. Ceriotti and J. Behler, *J. Phys. Chem. B.*, 2018, 122, 10158-10171.